OPEN ACCESS
Journal of Innovative Optical Health Sciences
Vol. 16, No. 3 (2023) 2250037 (11 pages)

DOI: 10.1142/S1793545822500377

World Scientific
www.worldscientific.com

Using optical coherence tomography images to evaluate fungal growth in reline resins

Mayra M. Aquino*,¶, Caio B. S. Maior†, Nathália A. E. Lins‡, Cláudia C. B. O. Mota‡, Patricia L. A. Nascimento‡ and Anderson S. L. Gomes§

*Graduate Program in Dentistry
Universidade Federal de Pernambuco (UFPE)
Recife, Brazil

†Center of Risk Analysis
Reliability Engineering and Environmental Modeling
Universidade Federal de Pernambuco (UFPE)
Recife, Brazil

‡Faculty of Dentistry
Centro Universitário Tabosa de Almeida (ASCES)
Caruaru, Brazil

§Department of Physics
Universidade Federal de Pernambuco (UFPE)
Recife, Brazil
¶mayra.aquino@ufpe.br

Received 13 March 2022
Revised 25 July 2022
Accepted 22 August 2022
Published 14 January 2023

As changes in hard or soft oral tissues normally have a microbiological component, it is important to develop diagnostic techniques that support clinical evaluation, without destroying microbiological formation. The optical coherence tomography (OCT) represents an alternative to analyze tissues and microorganisms without the need for processing. This imaging technique could be defined as a fast, real-time, *in situ*, and non-destructive method. Thus, this study proposed the use of the OCT to visualize biofilm by *Candida albicans* in reline resins for removable prostheses. Three reline resins (Silagum-Comfort, Coe-Comfort, and Soft-Confort), with distinct characteristics related to water sorption and fungal inhibition were used. A total of 30 samples (10 for each resin group) were subjected to OCT scanning before and 96 h after inoculation with *Candida albicans* (URM 6547). The biofilm analysis was carried out through a 2D optical Callisto SD-OCT (930 nm) operated in the spectral domain. Then, the images were preprocessed using a 3×3 Gaussian filter to remove the noise, and then Otsu binarization, allowing segmentation and pixel counting. The layer's biofilm formed was clearly defined and, indeed, its visualization is modified by water sorption of each material. Silagum-Comfort and Soft-Confort showed some similarities

in the scattering of light between the clean and inoculated samples, in which, the latter samples presented higher values of light signal intensity. Coe-Comfort samples were the only ones that showed no differences between the clean or inoculated images. Therefore, the results of this study suggest that OCT is a viable technique to visualize the biofilm in reline materials. Because findings in the literature are still scarcely using the OCT technique to visualize biofilm in reline resins, further studies are encouraged. It should not contain any references or displayed equations.

Keywords: OCT; reline resin; biofilm; removable prosthesis.

1. Introduction

In the late 19th century, the scientific community discovered that infectious diseases were caused by microorganisms.[1] Until recently, human microbiology was based on the identification of single microbes (e.g., bacteria, fungi, viruses) frequently isolated from patients with acute or chronic infections. Nowadays, new culture-independent molecular biochemical analyses allow the detection and classification of diverse microorganisms for a given ecosystem.[2]

Despite the technological advances, fundamental steps such as collecting and processing samples are still necessary to correctly identify the microorganism and to provide its specific treatment. In this context, according to the literature, several optical and non-optical imaging techniques have been previously developed for the study of microorganism structure and growth, such as Microscopy, magnetic resonance imaging (MRI), confocal laser scanning microscopy (CLSM), Raman microscopy, scanning electron microscopy (SEM), nuclear magnetic resonance imaging (NMRI), atomic force microscopy (AFM), and photoacoustic spectroscopy.[3,4] However, limitations associated with each approach may narrow its use in practice.

For example, despite SEM being often applied to visualize initial biofilm formation, it usually alters the original structure of biofilms.[4,5] More recently, CLSM has become one of the most used techniques, consisting of optical sectioning which acquires fluorescence signals only from a few hundred-nanometer thick focal plane within the sample.[6] Compared to normal or epifluorescence microscopy, CLSM has a significant advantage as the sample is scanned in 3D point-by-point, section-by-section, and slice-by-slice.[5] However, the requirements for cell labeling using CLSM limits its use on the study of natural biofilm *in vivo*, and shallow imaging penetration limits its application in the study of very thick biofilms.[4]

Non-optical techniques such as NMRI also were suggested to study cells and biofilms. NMRI, a non-invasive and non-destructive method, has been employed *in situ* but has low-image resolution and long acquisition times for images, once again limiting its application in biofilm monitoring in real-time.[7]

In this context, optical coherence tomography (OCT) represents an alternative to analyzing tissues and microorganisms without the need for processing or handling them. OCT is defined as a fast, real-time, *in situ*, and non-destructive imaging method that does not require any staining.[8] Indeed, recent studies suggest that OCT can be used to evaluate tissue alterations and microorganism presence on several surfaces.[5,9–11]

OCT explores a method similar to ultrasound imaging, once both technologies employ back-scattered signals reflected from within the tissue to reconstruct structural images, with OCT measuring light rather than sound.[8] The images are acquired using a flexible fiber-optic probe placed on the tissue to generate real-time surface and subsurface images of tissue microanatomy and cellular structure.[12] OCT generates a 2-dimensional, 1–10 μm resolution, and 2–3 mm depth image, representing the optical reflection within a tissue sample at near histologic resolution. In addition, these images can be stacked to generate 3-dimensional reconstructions of the target tissue.[13]

From successful applications in Ophthalmology, several investigations established that the OCT produces high-resolution images in distinct cases, inspiring its current use in other areas of Medicine and Dentistry.[14] Indeed, it provides images of biofilm, retina cells, pathological injuries, carious dental lesions, restoration failures, diagnosis of

periodontal diseases in studies *in vitro* and *in vivo*.[9,10,15–17]

In Dentistry, changes in hard or soft tissues normally have a microbiological component. In fact, thousands of bacterial and a hundred fungal phylotypes can colonize the oral cavity. Microbial communities colonize the mouth and grow in a biofilm,[13] which is defined as an aggregate of microorganisms growing within an extracellular polymeric and adherent matrix.[18,19] The matrix contains microbial metabolites, dead microbial, and host cells (i.e., desquamated epithelial cells), other host components (e.g., mainly fibronectin, laminin, collagen, and salivary constituents), food nutrients (sugars), and possibly also drugs. The matrix is well hydrated and crossed by channels conveying oxygen, nutrients, and metabolites.[13]

Although the main microbiological types presented in the oral cavity have already been identified, they cannot be noticed until the symbiosis between flora-individual is broken. Thus, the biofilm, when not disorganized or removed from the oral cavity, is responsible for the appearance of changes in oral tissues, such as periodontal disease, carious lesions, and prosthetic stomatitis.[20,21] Therefore, it is important to adopt non-invasive and non-destructive methods, like OCT, to visualize and control them.

Candida albicans is usually a harmless member of the native microbiota which asymptomatically colonizes several niches, including the gastrointestinal tract, reproductive tract, mouth, and skin. However, disturbances caused by shifts in pH, nutritional alterations, shifts in oxygen levels, antibiotic use, diseases, or immunosuppressant therapy can promote the over-proliferation of *Candida albicans*.[22] and often lead to severe symptoms. Studies have shown that a ubiquitous oral commensal of the mitis streptococcal group (*Streptococcus oralis*) has a mutualistic relationship with *Candida albicans* as it enables streptococcal biofilm growth at mucosal sites, and *Streptococcus oralis* facilitating the invasion of the oral and esophageal mucosa by *Candida albicans*.[23]

In addition, biofilms containing *Candida albicans* and *Streptococcus mutans* or *Streptococcus gordonii* are isolated from denture stomatitis. Regarding dental caries, although they have been associated primarily with Streptococcus mutans and Lactobacillus species, there is now growing evidence that *Candida albicans* actively participates in cariogenic biofilms, through synergistic interaction with *Streptococcus mutans*,[24] whereas *Candida albicans* and Pseudomonas aeruginosa are commonly co-isolated from skin and lung infections. These mixed-species biofilms can increase virulence and protect one or multiple species from environmental hazards. Moreover, *Candida albicans* infections range from superficial mucosal and dermal infections to disseminated bloodstream infections with mortality rates above 40%, particularly serious in immunocompromised individuals.[22]

There has been increasing evidence supporting that many systemic diseases (e.g., diabetes, cardiovascular diseases, and tumors) are associated with disturbances in the oral ecosystem. The current control of dental plaque-related diseases is nonspecific and centered on the removal of plaque by mechanical means.[25]

A diverse range of oral bacterial pathogens and bacterial DNA has been detected in atherosclerotic plaque. Indeed, pathogens from the mouth can access the atherosclerotic plaques via the bloodstream, promoting an inflammatory or immune response within the atherosclerotic plaque. Hence, the systemic inflammatory or immune response to periodontal infection may increase cardiovascular risk.[26,28] In addition, patients with diabetes mellitus have an increased risk of developing oral infections such as periodontal disease, while there also exist pieces of evidences suggesting that periodontal disease is a risk factor for the development of diabetes mellitus.[29] In this case, hyperglycemia enhances the expression of pathogen receptors, which enhance the host's response to the dysbiotic microbiome. Indeed, several pathogenic mechanisms that have true causal comorbidity are related to poorly controlled diabetes and periodontitis.[30]

Therefore, in this paper, the aim was to analyze the growth of *Candida albicans* on different surfaces, including reline resins for the base of removable prostheses, based on images obtained by OCT. Indeed, to the best of the author's knowledge, there is no work of this nature considering OCT to visualize microorganisms in acrylic or reline resins. The purpose is to identify whether the OCT is a viable imaging technique, non-invasive for biofilm visualizing, to understand his behavior and how could it be modulated, especially in materials used during

the treatment of infection oral diseases, which are part of the dental routine.

2. Material and Methods

2.1. *Reline resins*

Reline resins are divided into tissue conditioners and interim resilient liners. These materials are used in complete and partial removable dentures to distribute functional loads homogeneously on the denture-bearing tissue. In fact, reline resins can be divided into four groups according to their chemical structure: (i) Plasticized acrylic resins (self-curing and heat cure acrylic resins), (ii) vinyl resins, (iii) polyurethane, and (iv) silicone rubbers.[31]

Here, the behavior of three reline resins when infected by *Candida albicans* was analyzed.

2.2. *Experiment description*

A laboratory experimental study was performed analyzing three distinct brands of reline resins: One interim resilient liner based on polyvinylsiloxanee– Silagum Comfort (DMG, Hamburg, Germany) and two tissue conditioners — Coe-Comfort (Gc America, Alsip, USA) and Soft-Confort (Dencril, Pirassununga, Brazil). Each of the three reline resins groups was composed of 10 samples ($n = 10$). For the uniformity of the samples, a rectangular metal matrix was used, with dimensions of 64 mm × 10 mm × 2.5 mm. These materials are regulated by the American Dental Association.[32] The resins were processed and polished according to the guidelines of each manufacturer.

The samples were contaminated with *Candida albicans*, (URM 6547). Before inoculation, the inoculum was standardized to 108 colonies forming units/ml, equivalent to 0.5 Mac Farland scale.[33] The sterilized samples were placed in test tubes containing 3 mL of Sabouraud Dextrose (SD) broth and then inoculated with the 1 mL *Candida albicans* inoculum standardized.

From the 10 samples of each group, six were inoculated with *Candida albicans* and the other four were used for control. Considering the control group, two samples were immersed in broth without microorganisms, and the other two were immersed in water.

Despite the common use of 24–48 h for biofilm experiment, we designed ours to have 96 h duration to ensure cell adherence and the formation of a mature biofilm once the shaking step is not performed. Hence, all tubes were incubated in a microbiological oven for 96 h at 35°C. During this period, the culture medium was changed once, after 48 h, to retain the broth nutrients viable for biofilm formation. The change procedure consisted in removing 3 mL from the tube, which was incubated, and inserting 3 mL of new sterile culture medium SD broth. Then, at the end of 96 h, the samples were removed from the tubes using a tweezer, washed with sterile water, and let to dry off in Petri dishes until the OCT scanning. In addition, aliquots of the broth were removed and seeded in a solid culture Sabouraud Agar in Petri dishes being incubated for another 48 h to demonstrate the viability of the inoculum.

2.3. *OCT image scanning*

The samples and Petri dishes were submitted to OCT analysis in two moments: Before the inoculation, and after 96 h of culture of microorganisms. For resins samples, the employed OCT system (Callisto SD-OCT, Thorlabs Inc. Newton, New Jersey, United States) operated in the spectral domain, using a light source with 930 nm of central wavelength, with a maximum output power of 5 mW, axial resolution of 7/5.3 μm in water/air, lateral resolution of 8 μm, depth of light penetration of 1.6 mm inside the samples and provided images 2D with a numerical matrix of 1024 × 512 pixels. For the Petri dishes, the employed OCT system (OQ Labscope SD-OCT) also operated in the spectral domain, at a central wavelength of 840 nm as a light source and 0.75 mW of output power, lateral resolution of 15 μm; axial resolution of 7 μm in the air and 100 dB of sensitivity, capturing 12 images per second, constituting a numerical matrix of 512 × 512 pixels.

To obtain the images, reline samples and Petri dishes were positioned perpendicularly to the OCT handpiece, aiming to analyze the structural changes in the surface and inside both structures. Two-dimensional images were obtained by combining depth resolution and light scattering intensity profiles along the section of interest in the specimens. The generated images had pixels values ranging from 0 to 255 in a grayscale. Figure 1 presents the schematic diagram of the OCT for image generation.

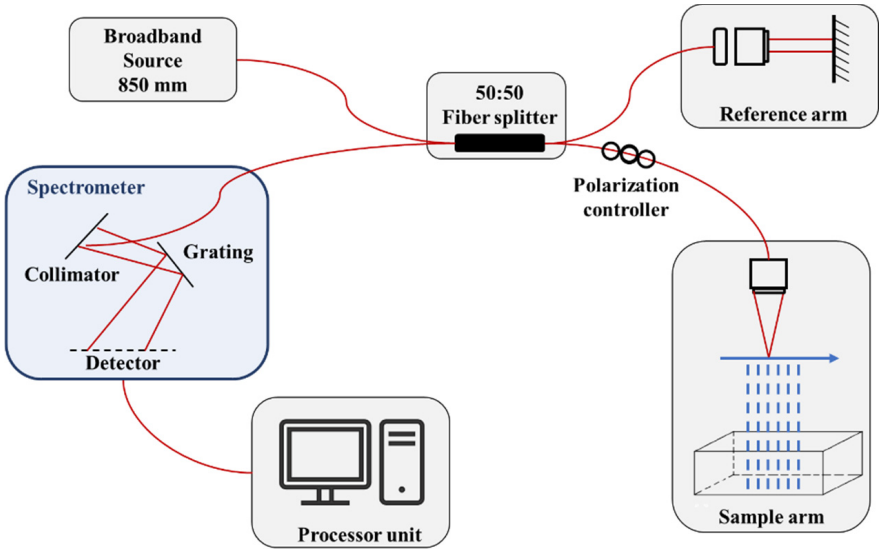

Fig. 1. Schematic diagram of the OCT imaging.

3. Results and Discussion

First, before inserting the resins, images from Petri dishes with sterile and inoculated mediums were collected (Fig. 2). Indeed, the images provided by OCT show clear differences in intensity, scattering, and penetration of light between them, simply by observation. The Petri dishes with fungal growth [Fig. 2(b)] have a thicker and stronger pattern than the ones with only culture medium Sabouraud Agar [Fig. 2(a)].

Then, each of the three reline resins was evaluated separately: (i) Silagum-Comfort, (ii) Coe-Comfort, and (iii) Soft-Confort. During the tests, to confirm the viability of the microorganisms inoculated, aliquots of the contaminated broth from each case were also added to the Petri dishes to grow.

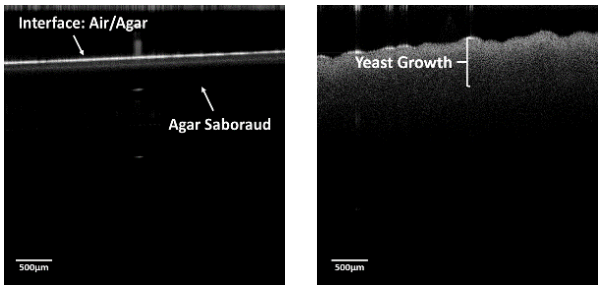

(a) (b)

Fig. 2. (a) Petri dishes contained sterile culture medium Sabouraud Agar; (b) Petri dishes contained standardized inoculum in Sabouraud Agar, where it presents *C. albicans* growth.

Here, a straightforward image processing was also performed to facilitate the visual differentiation. The aqueous environment biofilm is responsible for the necessity to apply a threshold to separate two structures in the image: the white pixels, that reflect the high signal intensity of the biofilm, and the black pixels of the aqueous environment itself. Firstly, pre-processed the images using a 3×3 Gaussian filter in order to remove the noise while retaining the important information. Indeed, filters based on Gaussian functions are of particular importance because their shapes are easily specified and both the forward and inverse Fourier transforms are real Gaussian functions.[34] Then, Otsu binarization[35] was applied to convert each pixel of the original image to a black or white value, and the number of white pixels in the binarized image was quantified. All images were processed using the "Open CV" package.[36] in Python programming language. In addition to the visual image qualitative assessment, the number of white pixels in each sample, which characterizes the signal strength, was quantified. The pixel counting for the three resins is depicted in Table 1.

The Silagum-Comfort is considered as an interim denture resilient material, derived from polyvinylsiloxane, which gives it better stability and tear resistance. Comparing images from non-contaminated initial samples [Fig. 3(a)] and the samples immersed in SD broth [Fig. 3(c)], no significant differences are perceived. Light scattering and intensity are similar, and the internal structure

Table 1. Number of white pixels after Otsu threshold application.

Resin	Initial image	Contaminated image
Silagum-Comfort	6091	68,868
Coe-Comfort	75,272	75,723
Soft-Confort	4965	24,401

also does not show relevant changes even in the samples immersed in the aqueous environment (SD broth) for 96 h, which demonstrates that this material has low water sorption.

From the sample contaminated with *Candida albicans*, presented in Fig. 3(e), one can see the biofilm as a well-defined area just below the sample surface. The presence of the microorganism seems to cause differences in the behavior of the relining resin and indicates that, in a favorable environment, this microorganism can not only adhere but also penetrate the materials. A second area of higher light intensity is also presented in the image, suggesting that in the deeper regions may exist a deposition of the broth components (dextrose and peptone), associated with the yeasts and their detritus.

The visualization is even easier after image processing [Figs. 3(b), 3(d) and 3(f)]. Indeed, considering the Silagum-Comfort case, the signal intensity is much higher in the inoculated samples than in clean samples.

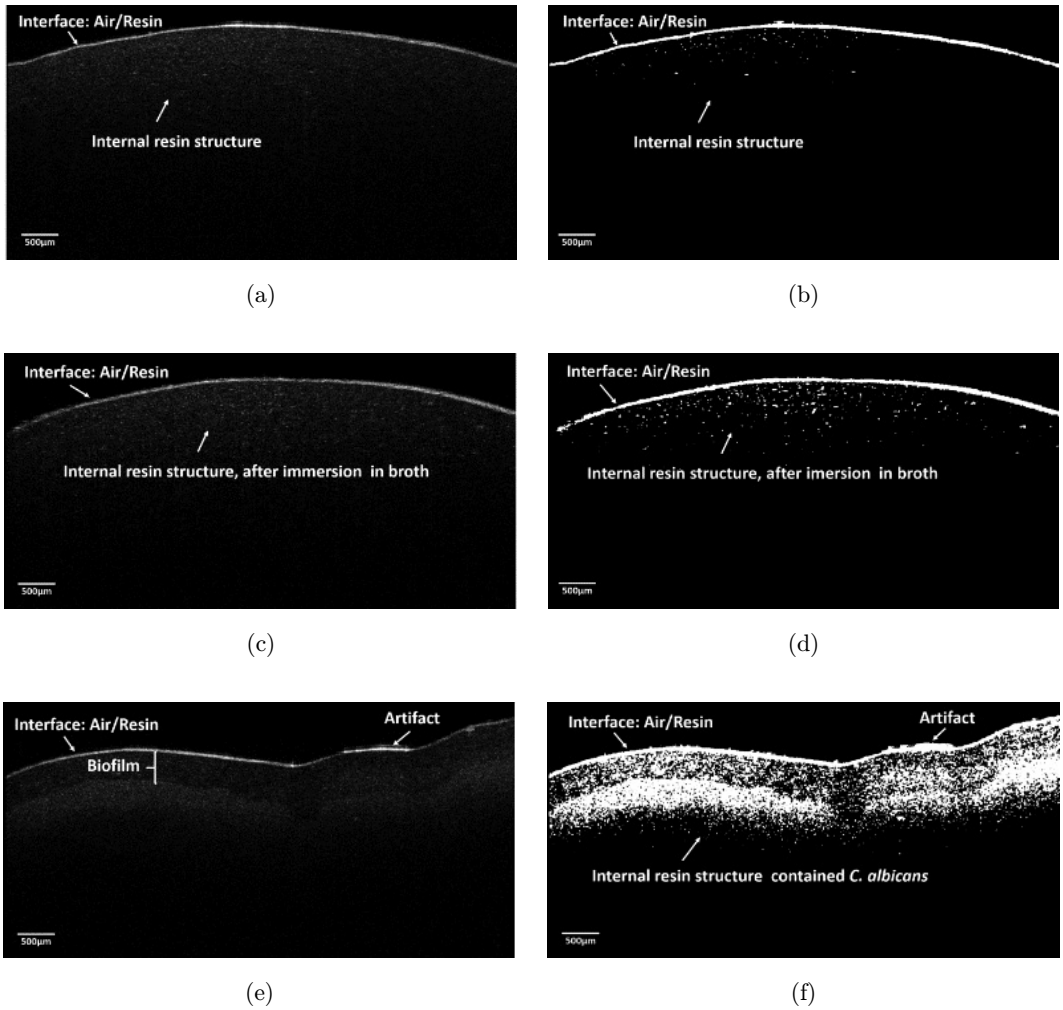

Fig. 3. OCT images obtained from Silagum-Comfort resin (a) Initial, sample clean and dry; (b) Initial sample after Otsu threshold; (c) Sample immersed in SD broth without microorganism — without differences from the first image; (d) Samples immersed in SD broth after Otsu threshold — small increase in light scattering, (e) 96 h after inoculation, showing an artifact caused by the presence of SD broth in sample during analysis in OCT and a well-defined area, evidencing presence of biofilm and culture medium; (f) sample with standardized inoculum *Candida albicans* after Otsu threshold, highest light scattering, two areas well-defined in the image: biofilm and culture medium.

Considering Coe-Comfort resins, the images from the sample before and after the inoculation do not show an easy differentiation between them [Figs. 4(a) and 4(e)]. Even after image processing [Figs. 4(b) and 4(f)], the differences are still not observed which is indeed confirmed after the white pixel counting (Table 1). This material contains in its composition zinc undecylenate, an antifungal component with a high molecular weight (431.91 g/mol), to prevent the formation of biofilm by *Candida albicans* in the samples. Thus, one notes the absence of alterations in the images indicating the non-growth of the microorganism, which confirms the antifungal effectiveness, at least, in the first 96 h of growth, and did not present significant alterations in water sorption.[37]

On the other hand, the Soft-Confort samples showed a less dense internal structure with larger pores [Fig. 5(a)]. After immersion in clean SD broth, this resin appears to have high water sorption, demonstrated by the increase in light penetration and intensity in the image. This water sorption is considerably high, causing the signal intensity to be stronger in the samples that contain only the clean broth [Fig. 5(c)]. As in other resins, when contaminated, Soft-Confort samples show a biofilm as a well-defined area, just below their surfaces, and a second area with significant signal intensity, however, in this case, the biofilm appears to be restricted only to superficial layers [Fig. 5(e)].

After the image processing, it is possible to confirm that the signal intensity is higher in samples

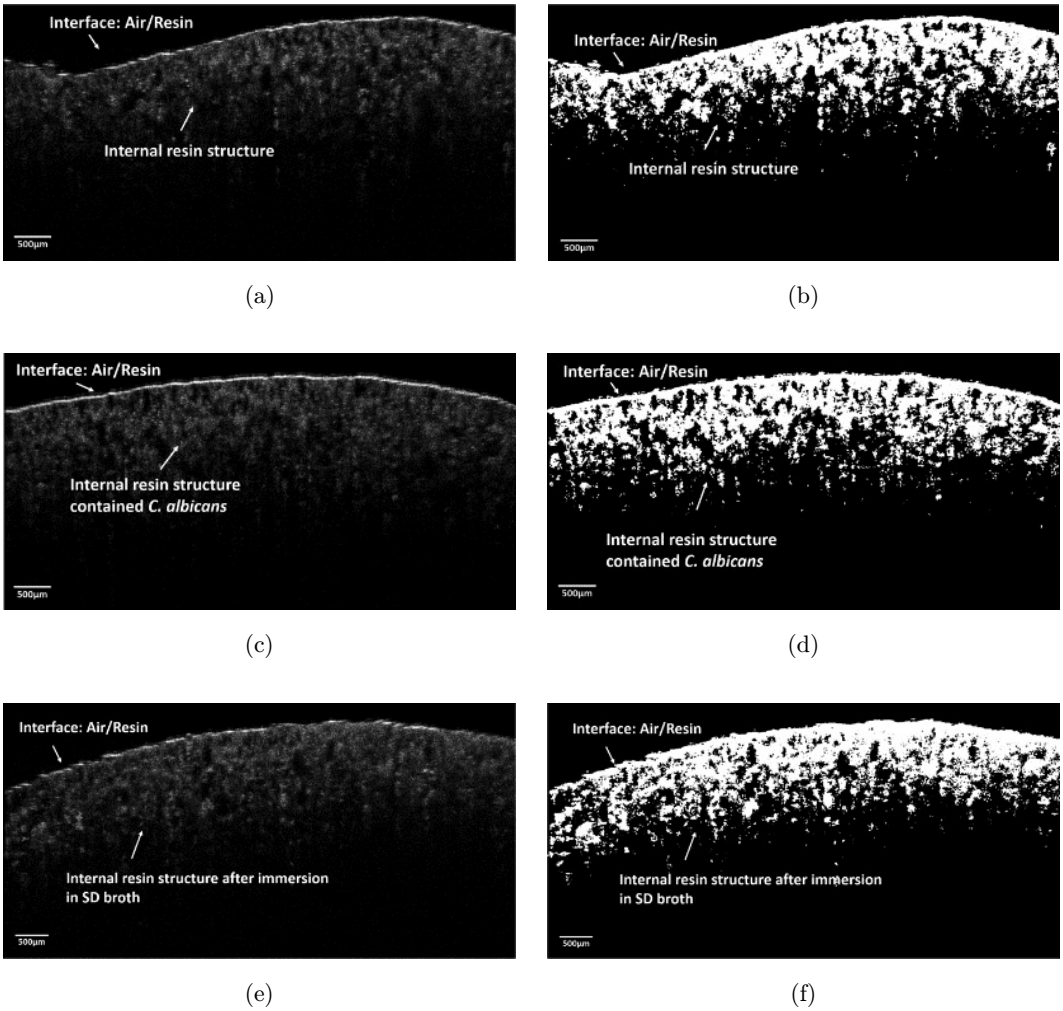

Fig. 4. OCT images obtained from Coe-Comfort resin (a) Clean sample before inoculation with *Candida albicans*; (b) clean sample after Otsu threshold; (c) clean sample immersed only in sterilized SD broth; (d) clean sample immersed in sterilized SD broth after Otsu threshold; (e) after inoculation with *Candidaalbicans*; (f) after inoculation with *Candida albicans* after Otsu threshold. No significant differences between images, even after image processing.

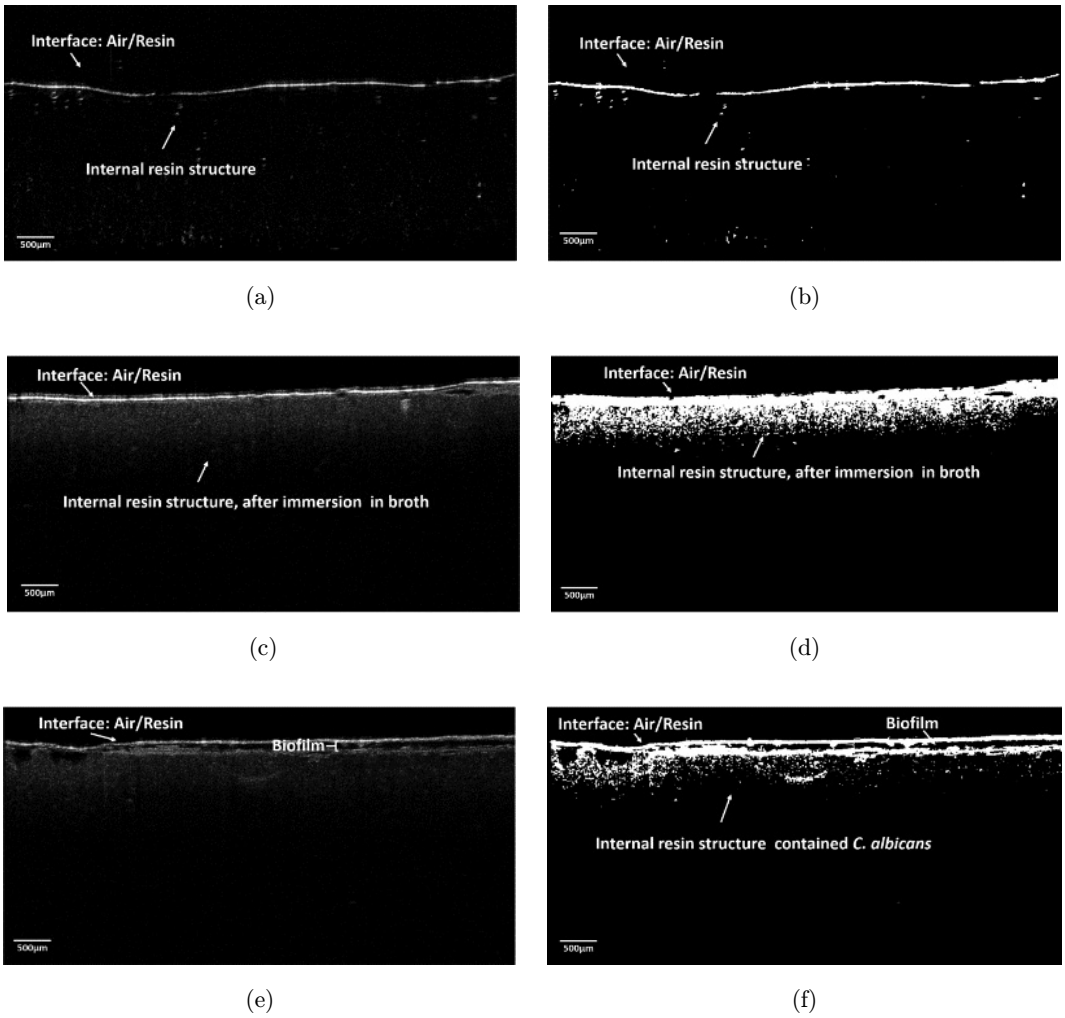

Fig. 5. OCT images obtained from Soft-Confort resin (a) Initial, clean and dry; (b) Initial after Otsu threshold; (c) immersed in sterilized SD broth without *Candida albicans*, however, is observed an increase in light scattering; (d) sample immersed in sterile SD broth, after Otsu threshold, it is noticed a higher light scattering and intensity; (e) sample contaminated after inoculation with *Candida albicans*; (f) sample contaminated by *Candida albicans*, with two areas well-defined: biofilm and culture medium; and with black spaces evidencing aqueous component of biofilm.

that are immersed only in clean broth than in contaminated samples [Figs. 5(b), 5(d) and 5(f)]. For proper validation, for each case (i.e., each reline resin), we also provide two more samples considering both initial and contaminated images as supplementary material.

Therefore, it is noticed that the resins Silagum-Comfort and Soft-Confort showed some similarities in the scattering of light between the clean and inoculated samples. However, the inoculated samples always presented higher values of light signal intensity because they actually include the presence of microorganisms and broth components. In this case, the distilled water penetrates and fills the temporary resin pores, transporting the broth components (dextrose and peptone) inside the sample (represented as an intense white area in the image). Despite that, in these inoculated samples, the biofilm is clearly seen just below the surface as a darkened area because it also contains water. Then, the black pixels that reflected low signals inside the biofilm may be seen as pores filled with water.

Related to water sorption, several factors are expected to influence how a plasticizer affects water transport in a glassy polymer.[38] Differences in the images are noticed when the Silagum-Comfort and Soft-Confort resin samples are immersed only in SD broth. For the Silagum-Comfort, which is considered an interim resilient liner based on polyvinylsiloxane, almost no differences in the light

scattering between the cleaned and immersed in broth samples are noticed, suggesting low levels of water sorption. On the other hand, Soft-Confort is considered an interim tissue conditioner based on plasticized acrylic resin, presenting extremely significant differences between cleaned and immersed in broth samples, suggesting higher levels of water sorption. Indeed, this result is in accordance with the literature, in which silicone elastomers (e.g., Silagum-Comfort) are reported to keep their properties for a longer period in contrast to the short-term ones (e.g., Soft-Confort).[39]

Thus, the real-time and non-destructive observation through OCT images allows the verification of the resin's behavior in the presence of biofilm and humid environment, providing data on the effectiveness of anti-fungal presence, water sorption and the relation between the type of material and biofilm growth. Moreover, the method may be replicated in other studies considering emerging strategies for modulating the oral microbiota such as in understanding the behavior of biofilm in the presence of silver nanoparticles and/or in new medications.

4. Conclusion

From the results, OCT is a viable technique for visualizing biofilm in reline resins. Indeed, in three tested resins, the microbiological growth is seen clearly in a non-destructive and non-invasive form. Moreover, the development of handheld OCTs aims to enable and facilitate the clinical use of the equipment in Dentistry as well as its dissemination.[40] Engineering and Dentistry studies also considered OCT as a method to identify the presence and behavior of the biofilm on distinct surfaces.[4,5,9] However, when applied to reline resins as the culture surfaces of biofilm, prior information about their compositions and physical characteristics of the surface (i.e., resin) is desirable for a better understanding related to the behavior in the aqueous environment (e.g., water sorption).

As a limitation, OCT does not provide data about the biofilm chemical composition, requiring previous knowledge about the structure. As findings in the literature are still scarcely using OCT technique to visualize biofilm in reline resins, further studies to compare and corroborate the results presented here are encouraged. In addition, in future works, machine and deep learning models to support the analysis of images (e.g., Maior *et al.*[41]) for OCT images in the Dentistry context will be considered.

Conflict of Interest

The authors declares have no conflicts of interest relevant to this article.

Acknowledgments

This study is a part of the INCT/INFO (National Institutes of Science and Technology, Photonics National Institute – 465.763/2014-6) and is supported by the CNPq/MCTI (National Council of Technological and Scientific Development and Ministry of Science Technology and Innovation), and the PRONEX program (Center of Excellence on Biophotonics and Nanophotonics – APQ-0504-1.05/14), sponsored by FACEPE/CNPq (Foundation for Science and Technology of Pernambuco State and National Council of Technological and Scientific Development).

References

1. D. P. Adams, *Foundations of Infectious Disease: A Public Health Perspective*, Jones and Bartlett Learning (2020).
2. H. E. Blum, "The human microbiome," *Adv. Med. Sci.* **62**, 414–420 (2017).
3. C. Li, S. Felz, M. Wagner, S. Lackner, H. Horn, "Investigating biofilm structure developing on carriers from lab-scale moving bed biofilm reactors based on light microscopy and optical coherence tomography," *Bioresour. Technol.* **200**, 128–136 (2016).
4. C. Xi, D. Marks, S. Schlachter, W. Luo, S. A. Boppart, "High-resolution three-dimensional imaging of biofilm development using optical coherence tomography," *J. Biomed. Opt.* **11**, 34001 (2006).
5. M. Wagner, H. Horn, "Optical coherence tomography in biofilm research: A comprehensive review," *Biotechnol. Bioeng.* **114**, 1386–1402 (2017).
6. M. Minsky, "Memoir on inventing the confocal scanning microscope," *Scanning* **10**, 128–138 (1988).
7. B. Manz, F. Volke, D. Goll, H. Horn, "Measuring local flow velocities and biofilm structure in biofilm systems with magnetic resonance imaging (MRI)," *Biotechnol. Bioeng.* **84**, 424–432 (2003).

8. D. Huang, E. A. Swanson, C. P. Lin, J. S. Schuman, W. G. Stinson, W. Chang *et al.*, "Optical coherence tomography," *Science* **254**, 1178–1181 (1991).
9. J. Hou, C. Wang, R. T. Rozenbaum, N. Gusnaniar, E. D. de Jong, W. Woudstra *et al.*, "Bacterial density and biofilm structure determined by optical coherence tomography," *Sci. Rep.* **9**, 9794 (2019).
10. J. Pattem, M. Davrandi, S. Aguayo, E. Allan, D. Spratt, L. Bozec, "A multi-scale biophysical approach to develop structure-property relationships in oral biofilms," *Sci. Rep.* **8**, 5691 (2018).
11. M. C. L. de Andrade, M. A. Soares De Oliveira, F. D. A. G. Dos Santos, P. D. B. Ximenes Vilela, M. N. Da Silva, D. P. C. Macêdo *et al.*, "A new approach by optical coherence tomography for elucidating biofilm formation by emergent Candida species," *PLoS One* **12**, e0188020 (2017).
12. P. Wilder-Smith, J. Holtzman, J. Epstein, A. Le, "Optical diagnostics in the oral cavity: An overview," *Oral Dis.* **16**, 717–728 (2010).
13. W. Jung, S. A. Boppart, "Optical coherence tomography for rapid tissue screening and directed histological sectioning," *Anal. Cell. Pathol.* **35**, 129–143 (2012).
14. G. L. Monroy, J. Won, "Clinical translation of handheld optical coherence tomography: Practical considerations and recent advancements," *J. Biomed. Opt.* **22**, 1–30 (2017).
15. W. Hadj-Saïd, N. Froger, I. Ivkovic, M. Jiménez-López, E. Dubus, J. Dégardin-Chicaud *et al.*, "Quantitative and topographical analysis of the losses of cone photoreceptors and retinal ganglion cells under taurine depletion," *Investig. Ophthalmol. Vis. Sci.* **57**, 4692–4703 (2016).
16. C. C. D. O. B. Mota, L. A. Gueiros, A. M. A. Maia, A. R. Santos-Silva, A. S. L. Gomes, F. D. A. Alves *et al.*, "Optical coherence tomography as an auxiliary tool for the screening of radiation-related caries," *Photomed. Laser Surg.* **31**, 301–306 (2013).
17. B. T. Amaechi, S. M. Higham, A. G. Podoleanu, J. A. Rogers, D. A. Jackson, "Use of optical coherence tomography for assessment of dental caries: Quantitative procedure," *J. Oral Rehabil.* **28**, 1092–1093 (2001).
18. M. Chevalier, S. Ranque, I. Prêcheur, "Oral fungal-bacterial biofilm models in vitro: A review," *Med. Mycol.* **56**, 653–667 (2018).
19. J. W. Costerton, P. S. Stewart, E. P. Greenberg, "Bacterial biofilms: A common cause of persistent infections," *Science* **284**, 1318–1322 (1999).
20. M. Károly, N. Gábor, N. Œdám, B. Andrea, "Characteristics, diagnosis and treatment of the most common bacterial diseases of the oral cavity," *Orv. Hetil.* **160**, 739–746 (2019).
21. H. Yumoto, K. Hirota, K. Hirao, M. Ninomiya, K. Murakami, H. Fujii *et al.*, "The pathogenic factors from oral streptococci for systemic diseases," *Int. J. Mol. Sci.* **20**, 4571 (2019).
22. M. B. Lohse, M. Gulati, A. D. Johnson, C. J. Nobile, "Development and regulation of single- and multi-species Candida albicans biofilms," *Nat. Rev. Microbiol.* **16**, 19–31 (2018).
23. M. Bertolini, A. Dongari-Bagtzoglou, "The Relationship of Candida albicans with the oral bacterial microbiome in health and disease," *Adv. Exp. Med. Biol.* **1197**, 69–78 (2019), doi: 10.1007/978-3-030-28524-1 _6.
24. K. Ellepola, Y. Liu, T. Cao, H. Koo, C. J. Seneviratne, "Bacterial GtfB augments Candida albicans accumulation in cross-kingdom biofilms," *J. Dent. Res.* **96**, 1129–1135 (2017).
25. Y. Zhang, X. Wang, H. Li, C. Ni, Z. Du, F. Yan, "Human oral microbiota and its modulation for oral health," *Biomed. Pharmacother.* **99**, 883–893 (2018).
26. R. Stewart, M. West, "Increasing evidence for an association between periodontitis and cardiovascular disease," *Circulation* **133**, 549–551 (2016).
27. S. Piconi, D. Trabattoni, C. Luraghi, E. Perilli, M. Borelli, M. Pacei *et al.*, "Treatment of periodontal disease results in improvements in endothelial dysfunction and reduction of the carotid intima-media thickness," *FASEB J.* **23**, 1196–1204 (2009).
28. S. J. Ott, N. E. El Mokhtari, M. Musfeldt, S. Hellmig, S. Freitag, A. Rehman *et al.*, "Detection of diverse bacterial signatures in atherosclerotic lesions of patients with coronary heart disease," *Circulation* **113**, 929–937 (2006).
29. P. P. Coll, A. Lindsay, J. Meng, A. Gopalakrishna, S. Raghavendra, P. Bysani *et al.*, "The prevention of infections in older adults: Oral health," *J. Am. Geriatr. Soc.* **68**, 411–416 (2020).
30. D. Polak, T. Sanui, F. Nishimura, L. Shapira, "Diabetes as a risk factor for periodontal disease—plausible mechanisms," *Periodontol 2000* **83**, 46–58 (2020).
31. K. Anusavice, R. Phillip, *Phillip's Science of Dental Materials*, Elsevier (2003).
32. ADA, "Revised American Dental Association specification No. 12 for denture base polymers," *J. Am. Dent. Assoc.* **90**, 451–458 (1975).
33. J. H. Jorgensen, M. A. Pfaller, K. C. Carroll, G. Funke, M. L. Landry, S. S. Richter *et al.*, *Manual of Clinical Microbiology*, ASM Press (2015), doi: 10.1128/9781555817381.
34. B. K. Shreyamsha Kumar, "Image denoising based on gaussian/bilateral filter and its method noise thresholding," *Signal Image Video Process.* **7**, 1159–1172 (2013).

35. N. Otsu, "A threshold selection method from gray-level histograms," *IEEE Trans. Syst. Man. Cybern.* **9**, 62–66 (1979).
36. G. Bradski, "The OpenCV library," *Dr Dobbs J. Softw. Tools* **120**, 122–125 (2000), doi: 10.1111/0023-8333.50.s1.10.
37. J. G. Maciel, C. Y. C. Sugio, G. C. C. Lamarque, A. L. F. Procópio, V. M. Urban, K. Neppelenbroek, "Determining acceptable limits for water sorption and solubility of interim denture resilient liners," *J. Prosthet. Dent.* **21**, 311–316 (2018).
38. S. Kalachandra, D. T. Turner, "Water sorption of plasticized denture acrylic lining materials," *Dent. Mater.* **5**, 161–164 (1989).
39. G. Zarb, J. Hobkirk, S. Eckert, R. Jacob, *Prosthodontic Treatment for Edentulous Patients — Complete Dentures and Implant-Supported Prostheses*, Mosby (2012).
40. J. Won, P.-C. Huang, D. R. Spillman, E. J. Chaney, R. Adam, M. Klukowska *et al.*, "Handheld optical coherence tomography for clinical assessment of dental plaque and gingiva," *J. Biomed. Opt.* **25**, 116011 (2020).
41. C. B. S. Maior, J. M. M. Santana, I. D. Lins, M. J. C. Moura, "Convolutional neural network model based on radiological images to support COVID-19 diagnosis: Evaluating database biases," *PLoS One* **16**, e0247839 (2021).